CDF/ANAL/EXOTIC/CDFR/6510
Version 1.0
June 23, 2003

XFT Efficiency for the Isolated Track Leg of the Electron+Track Trigger

S. Baroiant,[1] M. Chertok,[1] M. Goncharov,[2] T. Kamon,[2] V. Khotilovich,[2] R. Lander,[1] T. Ogawa,[3] C. Pagliarone,[4] G.M. Piacentino,[4] F. Ratnikov,[5] A. Safonov,[1] A. Savoy-Navarro,[6] J.R. Smith,[1] D. Toback,[2] S. Tourneur,[6] E. Vataga[4]

[1] University of California, Davis, [2] Texas A&M University,
[3] Waseda University, Japan, [4] INFN-Pisa, Italy, [5] Rutgers University,
[6] LPNHE-Universites de Paris 6 et 7/IN2P3-CNRS, France

Abstract

We present the L2 XFT trigger efficiencies for the track leg in the electron+track trigger. This track becomes a seed for hadronically decaying tau leptons. We measure the efficiency as a function of p_T, η and number of prongs for different run ranges. Before run 152636, at plateau region, the efficiency is found to be $97.7 \pm 0.4\%$ for the 1-prong case and $99.5 \pm 0.2\%$ for the 3-prong case. After the run 152636 the XFT requirements became tighter making the efficiency lower and no longer show a strongly pronounced plateau for high-p_T tracks. As a reference, at $p_T = 10$ GeV/c it is $93.5 \pm 0.6\%$ and $97.1 \pm 0.3\%$ for 1 and 3-prong cases correspondingly, still increasing with p_T. While the numbers above correspond to averaged track η-dependence, we separately perform a fit that explicitly takes it into account.

1 Introduction

The lepton+track trigger is a powerful tool for searching for physics beyond the SM in channels containing dilepton final states, especially final states where one of the leptons is a hadronically decaying tau [1]. The trigger was installed and commissioned in January 2002 and has since worked in a stable manner. The trigger efficiencies have been measured for the electron leg of the electron+track trigger at Level 1, Level 2 and Level 3 [2, 3]. Here we report on a study of the XFT trigger efficiencies for the isolated track leg of electron+track trigger[1] for different numbers of prongs (number of tracks in 10^o cone).

The note is organized as follows: we first give a brief description of the XFT and discuss the features which influence its performance in Section 2. In Section 3 we define the efficiency, followed by a description of the datasets used for its measurement in Section 4. In Section 5 we present the trigger cuts for XFT tracks and quality cuts for offline track selection. Section 6 gives details about the matching

[1] At present, there are no XFT trigger requirements for the isolated track leg in muon+track triggers. In the electron+track trigger the XFT information is used at Level 2 (XTRP).

between offline and XFT tracks. Results for 1D (in $1/p_T$) and 2D (in $1/p_T$ vs η space) efficiency dependencies are presented in Section 7. In Section 8 we look at the $W \rightarrow \tau\nu$ dataset as a cross-check with concluding remarks made in Section 9.

2 The XFT and COT

The XFT system is a part of the CDF Level 1 Trigger, and XFT tracks are used at both Level 1 and Level 2. The XFT trigger uses hits from axial ($r-\phi$) superlayers (no stereo information is used) of the COT and combines them into track segments at each superlayer, the segments then being linked together to produce the XFT tracks. For each track segment a certain number of found wire hits is required. The number of required hits was 10 (out of 12 possible) before run 152636 and 11 hits thereafter. These different XFT configurations are conventionally referred to as "2-miss" and "1-miss" respectively. The linking is performed by comparing the track segments with predefined roads (patterns). A track is reported by the XFT if 3 or 4 segments were successfully linked. In case of multiple XFT track candidates within one of ϕ-slices ($\Delta\phi = 1.25^o$) at SL6, the track with highest p_T is reported.

These special features of the XFT have to be properly taken into account when defining the trigger efficiency. Sometimes an XFT track can erroneously combine hits or segments from different tracks. In cases when several tracks are clustered together the XFT can "create" and report a higher p_T track than actually exists. Also, the ability of the XFT to build a track depends on the COT occupancy, the more active the COT is in some segment, the more likely XFT is to find a track at all. Thus, when there are lots of tracks, not only is the XFT more likely to reconstruct tracks, but it is more likely to have its reported tracks be high p_T. As the isolated track of the electron+track trigger is expected to become a seed track of a tau candidate, which often has several prongs in a narrow cone, these "collective" effects are important and the definition of the efficiency should properly handle such cases.

There are also several effects associated with the mechanical design of the COT chamber. First of all, an XFT track can successfully be found only if the particle passes through all four axial superlayers. This means that during the offline tracks selection we require them to be inside of the fiducial volume of the XFT. Another geometry related effect is that the XFT performs worse for the low η tracks, the shorter path length inside of COT gives smaller charges collected by wires and thus a lower probability to produce a hit. Also, at $z = 0$ (right in the middle of the detector), a special structure called "the spacer" supports the COT wires. When a track passes through the spacer, it is less likely to produce hits in the region of small z. One or two lost hits can result in a not reconstructed segment, and the whole XFT track will not be found. This η-dependence of the XFT efficiency becomes especially pronounced for low p_T tracks, since low p_T particles produce weaker ionization, decreasing the probability of generating a COT hit, so the efficiency decreases.

During the January 2003 shutdown the COT voltage was changed, and we also compare the XFT efficiency for data before and after the shutdown. Lower HV on the wires results in smaller showers and smaller gains on the wires, leading to smaller signals and less chance to pass the pre-TDC discriminator thresholds. If two hits are lost at the same superlayer, the whole XFT track will not be reconstructed. Loosing two hits was not very unlikely number even with the pre-shutdown conditions, and even relatively small changes could make losses larger.

3 Efficiency Definition

For the track-leg of the electron+track trigger we define the XFT efficiency as

$$Efficiency = \frac{number\ of\ good\ isolated\ tracks\ with\ a\ triggered\ XFT\ match}{number\ of\ good\ isolated\ tracks}, \quad (1)$$

where *good isolated tracks* means that we have applied certain quality cuts for offline tracks, and *triggered XFT match* means that they have corresponding XFT tracks which passed trigger cuts. The track selection and matching procedures should properly take into account the discussed above effects. Section 5 describes the procedure for the track selection and the offline track to XFT track matching method is presented in Section 6. The matching is of particular concern here as the main purpose of the isolated track leg of the lepton+track trigger is that it can result in a reconstructed tau candidate [1], and we cannot use the matching technique which is based on comparison of helices, because due to XFT irregularities an offline track could have an XFT "partner" with a dissimilar set of helix parameters. Therefore, it is better to think about the XFT efficiency as an average probability that the presence of a given track triggers the XFT, which is dependent on the density of COT hits. If we had access to the information about XFT track's hits, then we would be able to check if the fraction of hits it shares with the original track is significant. Unfortunately, it is not possible as the TL2D bank does not have this information. To take this into account our matching is done for a tau-like combinations of tracks in a 10^o sector centered on an isolated track under consideration as a seed track. The matching is simple in this case: we check if there is any triggered XFT track inside the sector, and we use the number of prongs in our tau-like object to parametrize the COT activity as it is a convenient analysis variable (see Section 6 for a more detailed description of matching).

It should be noted that for the 1-prong case our results can be used for any analysis in which the isolated track leg of the electron+track trigger is expected to become an isolated electron or muon, as we don't require any special tau ID cuts except track isolation and track quality.

4 Datasets

For measuring the XFT trigger efficiency we created three data samples, summarized in Table 1. We stripped events from jet datasets choosing good runs with high statistics where we require at least one electron object with loose electron cuts (default EmObject cuts). This data does not have any bias from XFT triggers.

5 Trigger Requirements and Offline Track Selection

The trigger requirements for the ISOTrack in the Electron+Track trigger are given in Table 2. In this study a good isolated track is considered to pass the trigger if the matched XFT track parameters satisfy L2 cuts 1 and 2. We can then study the efficiency as a function of the offline p_T and η. To get the XFT track ϕ_6 (the ϕ position of the track in the middle of COT superlayer number 6) and p_T (which is obtained from the number of the curvature bins) we use the TL2D bank .

We get the offline tracks from the $defTracks$ view and apply additional quality and fiduciality requirements for each track to ensure that track can be expected to trigger the XFT if the XFT system is

Table 1: The data samples used for measuring the XFT trigger efficiencies from jet data. Note that before run 152636 XFT segment required at least 10 (out of 12) hits to be found ("2 misses"), and after the XFT was switched to a "1-miss" configuration. After the January 2003 shutdown, the COT voltage was lowered.

D/S label	dataset name and run numbers range	max number of missing hits allowed	before Jan.2003 shutdown	number of stripped events
A	gjet08: 151476-152615	2	yes	156 K
B	gjet08: 152674-153416	1	yes	169 K
C	gjet09: 160151-160761	1	no	266 K

Table 2: Requirements for the ISOTrack part in the Electron+Track trigger. In this study we apply cuts 1 and 2 at Level 2.

Trigger	Trigger Cuts
Level 1	no requirements
Level 2	**1)** $\mathbf{p_{T\ XFT} \geq 5.18}$ GeV/c**;** **2) XFT track has 4 layers;** 3) $\Delta\phi_6(e, trk) \geq 10^o$;
Level 3	$p_T \geq 5$ GeV/c; $\lvert\eta\rvert \leq 1.5$; no other tracks with $p_T > 1.5$ GeV/c and $\lvert z_0(seed) - z_0(trk)\rvert < 15$ cm within $0.175 \leq \Delta R \leq 0.524$; $\lvert z_0(e) - z_0(trk)\rvert \leq 15$ cm; $\Delta R(e, trk) \geq 0.175$.

fully efficient. Table 3 presents both requirements, as well as the track based tau ID emulation cuts (seed and isolation requirements) that we have used for offline track selection. We assume that electron and tau legs of the trigger are independent. However, we use some of the L3 cuts here, including the electron-track topology requirements to select events better resembling the targeted physics signal. Also, we repeat the efficiency calculation for a sample with no requirement of a partner electron. This "unbiased" sample has larger statistics and serves as a cross-check to verify the assumption of the two trigger legs (electron and track) being uncorrelated.

In our study we use the three dimensional tau-like offline track isolation (the same as in the L3 electron+track trigger). In addition we check the case of an additional 2D isolation requirement in the segment $\Delta\phi < 10^o$ excluding the $\Delta\Theta < 10^o$ tau-cone (see Fig. 1) as it helps to estimate a lower bound or "pure" XFT efficiency. Such additional isolation ensures that the XFT, which works in two dimensions, deals only with tracks from our 10^o tau-cone inside the $\Delta\phi < 10^o$ segment. The COT environment for the jet data is in general busier then for typical events which pass the Electron+Track trigger, so it is interesting to have an estimate from cleaner events. Also, this requirement automatically satisfies the third L2 cut in Table 2. We consider this efficiency as a lower bound for the efficiency: the fewer hits there are in some COT segment, the harder is the track reconstruction task for the XFT.

Table 3: Offline track selection cuts. $R_{2(8)}$ is the radius of the center of the first (last) axial superlayer. $\Delta\Theta$ denotes a 3D angle around the seed track (as in a standard τ reconstruction).

Track quality cuts:	$p_T > 3$ GeV/c; $\|\eta\| \leq 1.5$; $N_{axialCThits} \geq 25$, $N_{stereoCThits} \geq 25$; $\|d_{0corr}\| < 0.2$ cm;
fiducial region for XFT requirements:	$\|z_{COT}(R = R_2)\| < 150$ cm, $\|z_{COT}(R = R_8)\| < 150$ cm;
seed track requirement:	has the highest p_T among the tracks within $\|\Delta z_0\| < 15$ cm in its 10^o cone;
tau-like isolation, two cases:	a) no tracks with $p_T > 1.5$ GeV/c and $\|z_0(seed) - z_0(trk)\| < 15$ cm within the cone $10^o < \Delta\Theta < 30^o$ around the seed track; b) in addition to a) no tracks with $p_T > 1.5$ GeV/c within the segment $\Delta\phi < 10^o$ around the seed track except for those in the 10^o tau-cone (see Fig. 1);
electron partner requirement cuts:	$\|z_0(e) - z_0(trk)\| \leq 15$ cm; $\Delta R(e, trk) \geq 0.175$.

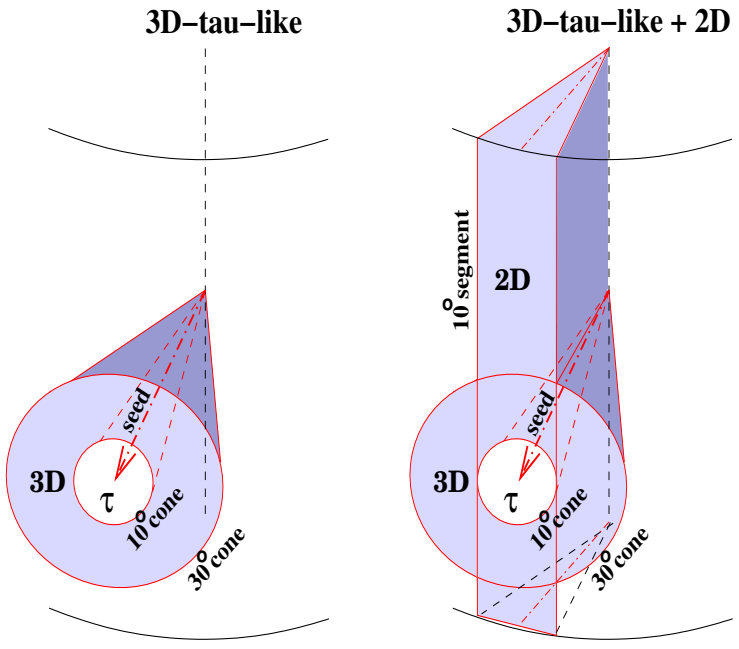

Figure 1: Illustration of the two kinds of tau-like isolation (see Table 3): 3D-tau-like and with additional isolation in the segment $\Delta\phi < 10^o$. The isolation areas are colored.

6 Matching of Offline and XFT tracks

The standard matching algorithm between offline and XFT tracks is described in Ref. [4]. The algorithm propagates both the XFT and the offline tracks to each of four axial superlayers and requires that the two positions are within 10 pixels of each other for each superlayer. A track is called "matched" if at least three out of four superlayers pass this requirement. The standard method [4] offers a reasonable trade-off between a comparison of helices and allowing for XFT irregularities, and we have checked that the 10-pixel cut is an acceptable difference at a given layer (see Fig. 2). This method works well for electrons and muons, but for taus, which can have several tracks, another approach is better. We ask the question "was there any XFT track which triggered the event for a given tau?" Exact matching is not needed here, as the tau could have several tracks.

For taus we developed the following matching procedure:

- count the number of prongs (tracks with $p_T > 1$ GeV/c in a 10^o cone) for every track which passes quality cuts,
- check every track to see if it is the seed track (has the highest p_T in the cone),
- for the seed track, look for a triggered XFT track in the 2D 10^o sector (using the ϕ_0 values for XFT tracks which can be found by extrapolating them from SL6 to the beam axis),
- we have a match if any XFT track is found.

We find that we can use the number of prongs in our "tau" as a convenient measure of COT activity and classify the efficiency accordingly.

7 Results

In this Section we will present the fit results for the XFT efficiency as a function of $1/p_T$ (Subsection 7.1) and as a function of $1/p_T$ and η (Subsection 7.2). Since real tau seed tracks may have slightly different η distribution, having η-dependent parametrization is helpful. But we note that the averaged out η-dependence is useful, as it allows direct comparison of the samples, makes it more easy to observe basic trends and gives a possibility to check if our efficiency parametrization in two dimensional ($1/p_T$ vs. η) space is good.

7.1 Efficiency parametrization as a function of $1/p_T$ only

In this section we assume that η-dependence is properly averaged out. We fit the XFT efficiency using the following parametrization (this formula can be easily obtained from the error function and the assumption that the curvature resolution is constant as a function of curvature):

$$\epsilon(1/p_T) = K_\infty \times freq\left(\frac{1/p_{T_0} - 1/p_T}{2\sigma_{p_T}}\right), \tag{2}$$

where p_T is the transverse momentum of the seed track, K_∞ is the asymptotic limit of the efficiency, p_{T_0} is the middle of the turn-on region and σ_{p_T} is the XFT curvature resolution. Results of a binned likelihood fit for $1/p_T$ distributions for the data sample A for different number of prongs, isolation type and electron requirement are presented in Table 4, and Figure 3 shows the efficiencies as functions of $1/p_T$ for this data sample. We perform fitting in the region $0 < 1/p_T < 1/4.5$ GeV/c.

Table 4: Results of the 3-parameter (Eq.2) fit of the XFT track finding efficiency for different requirements for electron and isolation for data sample A. K_∞ is measured in %, p_{T_0} in GeV/c and $\sigma_{p_{T0}}$ in $(100 \times \mathrm{GeV}/c)^{-1}$.

Ele. req.	ISO type		number of prongs					
			1	2	3	4	5	any
yes	3D	K_∞	97.72±0.41	98.97±0.26	99.46±0.18	99.48±0.18	99.69±0.16	99.35±0.08
		p_{T_0}	4.77±0.02	4.71±0.03	4.63±0.04	4.49±0.08	4.27±0.16	4.64±0.02
		$\sigma_{p_{T0}}$	0.92±0.07	1.08±0.11	1.09±0.16	1.26±0.26	1.72±0.46	1.15±0.06
	+2D	K_∞	97.72±0.43	98.91±0.31	99.28±0.26	99.54±0.21	99.72±0.21	99.18±0.11
		p_{T_0}	4.79±0.02	4.72±0.03	4.59±0.07	4.56±0.08	4.17±0.29	4.69±0.02
		$\sigma_{p_{T0}}$	0.89±0.07	1.14±0.14	1.45±0.25	1.17±0.26	2.16±0.88	1.14±0.07
no	3D	K_∞	98.08±0.27	99.09±0.18	99.33±0.15	99.58±0.13	99.72±0.11	99.37±0.06
		p_{T_0}	4.75±0.02	4.72±0.02	4.64±0.03	4.51±0.05	4.42±0.08	4.63±0.01
		$\sigma_{p_{T0}}$	1.01±0.06	1.06±0.08	1.11±0.11	1.42±0.18	1.43±0.23	1.18±0.05
	+2D	K_∞	97.95±0.32	98.86±0.23	99.22±0.19	99.59±0.15	99.71±0.15	99.22±0.08
		p_{T_0}	4.79±0.01	4.74±0.02	4.63±0.04	4.51±0.07	4.41±0.11	4.68±0.01
		$\sigma_{p_{T0}}$	0.96±0.06	1.08±0.09	1.22±0.14	1.55±0.22	1.50±0.33	1.16±0.05

For data for which the XFT allowed only one missing hit (samples B and C), the trigger efficiency acquires a non-negligible p_T dependence. This can be accounted for by introducing a forth parameter, S, and the parametrization:

$$\epsilon(1/p_T) = (1 - S\,(1/p_T - 1/10)) \times K_{10} \times freq\left(\frac{1/p_{T_0} - 1/p_T}{2\sigma_{p_T}}\right), \tag{3}$$

where S is the slope of the efficiency at high p_T and K_{10} is the efficiency[2] at $p_T = 10\ \mathrm{GeV}/c$. We have chosen this parametrization because K_{10} can be directly compared to the parameter K_∞ of the 3-parameter fit 2, while parameters S and K_{10} remain almost uncorrelated. More "intuitive" forms with asymptotic K either require one additional parameter or lead to a strong correlation between the normalization and the slope. The fit results are summarized in Tables 5 and 6, while Figures 4 and 5 show the efficiencies as functions of $1/p_T$ for the data samples B and C respectively. For sample A the efficiency itself is high and the slope is negligible, so we use the parametrization without slope (Eq.(2)).

Some of the plots show that there is some inefficiency in the $p_T > 20\ \mathrm{GeV}/c$ region. We checked what causes it and the reasons were the following: in approximately 50% of cases the failures occurred if tracks passed through the central spacer, in 25% the XFT track had only 3 out of 4 layers and for the remaining 25% the XFT did not reconstruct any tracks in the neighborhood of the seed track. Also the visual effect of fluctuations in the efficiency in the high-p_T region is greater because of the low statistics there.

[2] K_{10} is not the exact efficiency at $p_T = 10\ \mathrm{GeV}/c$, but is very close to it as the frequency function in the eq. (3) at this point is very close to one.

Table 5: Results of the 4-parameter (Eq.3) fit of the XFT track finding efficiency for different requirements for electron and isolation for data sample B. K_{10} is measured in %, p_{T_0} in GeV/c, $\sigma_{p_{T0}}$ in $(100 \times \mathrm{GeV}/c)^{-1}$ and S in GeV/c.

Ele. req.	ISO type		number of prongs					
			1	2	3	4	5	any
yes	3D	K_{10}	94.19±0.65	95.69±0.48	96.17±0.44	97.81±0.36	98.96±0.29	97.29±0.15
		p_{T_0}	4.88±0.02	4.81±0.02	4.76±0.03	4.67±0.05	4.59±0.06	4.76±0.01
		$\sigma_{p_{T0}}$	0.83±0.07	0.99±0.11	1.00±0.14	1.14±0.19	1.24±0.23	1.08±0.06
		S	4.55±1.40	2.30±1.12	2.55±0.96	1.33±0.80	1.32±0.51	2.65±0.28
	+2D	K_{10}	94.36±0.66	95.66±0.53	96.25±0.52	97.50±0.47	98.86±0.40	96.80±0.20
		p_{T_0}	4.89±0.02	4.84±0.03	4.76±0.04	4.65±0.06	4.51±0.13	4.80±0.01
		$\sigma_{p_{T0}}$	0.79±0.07	1.01±0.12	1.07±0.20	1.10±0.23	1.45±0.44	1.00±0.06
		S	4.69±1.36	2.23±1.21	2.27±1.16	1.23±1.10	1.34±0.75	3.06±0.36
no	3D	K_{10}	94.65±0.44	95.65±0.36	96.39±0.32	97.86±0.26	98.75±0.23	97.30±0.11
		p_{T_0}	4.88±0.01	4.83±0.02	4.76±0.02	4.69±0.03	4.59±0.05	4.76±0.01
		$\sigma_{p_{T0}}$	0.89±0.06	0.95±0.07	1.11±0.11	1.16±0.12	1.28±0.18	1.08±0.04
		S	3.11±0.94	2.64±0.80	2.20±0.76	1.58±0.59	1.29±0.41	2.48±0.21
	+2D	K_{10}	93.91±0.57	95.59±0.39	96.30±0.37	97.39±0.34	98.60±0.31	96.80±0.15
		p_{T_0}	4.91±0.01	4.86±0.02	4.77±0.03	4.69±0.04	4.50±0.09	4.81±0.01
		$\sigma_{p_{T0}}$	0.82±0.06	0.94±0.08	1.15±0.13	1.08±0.14	1.49±0.32	1.01±0.04
		S	2.98±1.23	2.58±0.88	2.26±0.90	1.75±0.79	1.25±0.59	2.88±0.28

7.1.1 Discussion

Figure 6 summarizes the dependence of the plateau efficiency (or the efficiency at $p_T = 10$ GeV/c) on number of prongs. As explained in Section 2, the increase in the efficiency is expected when we have more close tracks. The special features of the XFT also explain the residual efficiency under the trigger threshold (low p_T regions in Figures 3, 4 and 5). It causes the XFT "resolution" for p_T, $\sigma_{p_{T0}}$, to become worse and the middle of the turn-on region to shift to lower p_T as we have more prongs and tracks are "promoted" to higher p_T. Especially for the 5-prong case $\sigma_{p_{T0}}$ is noticeably larger, as the residual efficiency becomes really high and the turn-on step becomes low and smeared.

As already mentioned in Section 5, the efficiency is always lower when we require additional 2D isolation than when we have only the usual 3D-tau-like one (see Fig. 6). The efficiencies are similar for samples with and without requirement of an electron partner.

Figure 6d shows how the data samples A, B and C compare. The plateau efficiencies for the pre and after run 152636 data are quite different, as expected because of the tighter number of hits requirement. For the samples B and C they are similar but some systematic difference cannot be excluded.

7.2 Efficiency parametrization as a function of $1/p_T$ and η

Due to the COT geometry the XFT efficiency depends on η. Figure 7 shows it as a function of η and demonstrates an inefficiency at low η. We use a 3-parameter gaussian-like parametrization of the

Table 6: Results of the 4-parameter (Eq.3) fit of the XFT track finding efficiency for different requirements for electron and isolation for data sample C. K_{10} is measured in %, p_{T_0} in GeV/c, $\sigma_{p_{T0}}$ in $(100 \times$ GeV/$c)^{-1}$ and S in GeV/c.

Ele. req.	ISO type		number of prongs					
			1	2	3	4	5	any
yes	3D	K_{10}	93.46±0.60	95.73±0.40	97.06±0.32	97.95±0.31	98.99±0.33	97.41±0.12
		p_{T_0}	4.89±0.02	4.84±0.02	4.78±0.02	4.67±0.04	4.40±0.13	4.76±0.01
		$\sigma_{p_{T0}}$	0.95±0.07	1.01±0.08	1.06±0.11	1.30±0.19	2.01±0.54	1.15±0.05
		S	2.98±1.42	1.02±0.97	3.05±0.60	1.63±0.54	0.63±0.62	2.46±0.22
	+2D	K_{10}	93.19±0.64	94.92±0.47	96.62±0.40	97.56±0.38	98.57±0.40	96.65±0.17
		p_{T_0}	4.90±0.02	4.85±0.02	4.79±0.03	4.68±0.05	4.51±0.14	4.82±0.01
		$\sigma_{p_{T0}}$	0.85±0.06	1.01±0.09	1.12±0.13	1.14±0.23	1.49±0.56	1.03±0.05
		S	2.92±1.51	1.71±1.10	3.56±0.73	2.15±0.73	0.98±0.62	3.17±0.29
no	3D	K_{10}	94.27±0.37	95.77±0.30	96.98±0.23	97.81±0.22	98.59±0.20	97.36±0.09
		p_{T_0}	4.86±0.01	4.84±0.01	4.77±0.02	4.71±0.03	4.58±0.05	4.76±0.01
		$\sigma_{p_{T0}}$	0.95±0.05	1.02±0.06	1.08±0.08	1.21±0.11	1.36±0.17	1.12±0.03
		S	3.79±0.87	0.89±0.74	2.72±0.52	1.54±0.46	1.08±0.39	2.38±0.18
	+2D	K_{10}	93.06±0.51	95.18±0.34	96.68±0.28	97.35±0.28	98.34±0.28	96.72±0.12
		p_{T_0}	4.90±0.01	4.86±0.02	4.78±0.02	4.69±0.03	4.59±0.06	4.81±0.01
		$\sigma_{p_{T0}}$	0.84±0.05	1.02±0.07	1.10±0.09	1.17±0.14	1.25±0.25	1.04±0.03
		S	2.40±1.19	1.15±0.83	3.00±0.62	1.96±0.62	1.15±0.48	2.79±0.24

efficiency to take this dependence in account:

$$\epsilon(\eta) = K_\eta \times \left(1 - C_\eta \exp\left(-\frac{\eta^2}{2\sigma_\eta^2}\right)\right), \tag{4}$$

where C_η is the Gaussian height and σ_η is the Gaussian width (see Fig. 7). We also note that the depth of the dip at small η depends on the p_T of the tracks contributing to the sample, being smaller for higher p_T tracks and larger (larger inefficiency) for soft tracks. To properly account for these effects we use the following parametrization:

$$\epsilon(1/p_T, \eta) = K_\infty \times freq\left(\frac{1/p_{T_0} - 1/p_T}{2\sigma_{p_T}}\right) \times \left(1 - C_\eta \times 1/p_T \times \exp\left(-\frac{\eta^2}{2\sigma_\eta^2}\right)\right). \tag{5}$$

If compared to Eq.(3), one may note that the effective slope is still present and comes from the η-dependent gaussian portion. The results of the 5-parameter fits in the region $0 < 1/p_T < 1/4.5$ GeV/c, $|\eta| < 1.4$ are presented in Tables 7, 8 and 9 and Figure 8. As a cross-check we perform the following test: we start with the original distribution of the tracks; for all tracks in each p_T bin we use the efficiency obtained using Eq.(5) to predict the number of tracks which pass the "trigger". We then divide one distribution by another and fit it using Eq.(3). The result is consistent with original fits (Tables 5 and 6) proving that we correctly account for the η dependence and the correlation of $1/p_T$ and η. One can also verify this by integrating out the η-dependent gaussian part and assuming that initial η distribution of tracks is approximately flat in the region of $|\eta| < 1$, which gives $\sqrt{2\pi}C_\eta\sigma_\eta/(\eta_{max} - \eta_{min}) \approx S$.

Table 7: Results of the 5-parameter (Eq.5) fit of the XFT track finding efficiency for different requirements for electron and isolation for data sample A. K_∞ is measured in %, p_{T_0} in GeV/c , $\sigma_{p_{T0}}$ in $(100 \times \mathrm{GeV}/c)^{-1}$, C_η in $(0.1 \times \mathrm{GeV}/c)$ and σ_η in $0.1 \times$ *inversed units of rapidity*.

Ele. req.	ISO type		number of prongs					
			1	2	3	4	5	any
yes	3D	K_∞	$99.84^{+0.16}_{-0.37}$	$99.99^{+0.01}_{-0.85}$	$99.90^{+0.10}_{-0.18}$	99.87±0.13	$99.92^{+0.08}_{-0.11}$	99.92±0.05
		p_{T_0}	4.75±0.02	4.70±0.02	4.59±0.04	4.47±0.06	4.40±0.09	4.62±0.01
		$\sigma_{p_{T0}}$	0.94±0.06	1.06±0.09	1.18±0.14	1.34±0.21	1.33±0.29	1.15±0.05
		C_η	3.64±0.82	2.70±0.77	1.04±0.52	1.61±0.86	1.22±0.79	1.99±0.31
		σ_η	3.01±0.57	2.76±0.63	3.56±1.57	1.99±0.65	2.44±0.88	2.67±0.30
	+2D	K_∞	$99.96^{+0.04}_{-0.57}$	$99.99^{+0.01}_{-2.59}$	99.71±0.29	$99.88^{+0.12}_{-0.19}$	$100.00_{-0.14}$	99.92±0.08
		p_{T_0}	4.78±0.02	4.72±0.03	4.60±0.05	4.55±0.06	4.35±0.14	4.68±0.01
		$\sigma_{p_{T0}}$	0.90±0.06	1.11±0.11	1.36±0.21	1.19±0.21	1.51±0.47	1.10±0.05
		C_η	4.27±0.91	2.60±0.82	1.49±0.89	1.06±0.75	1.52±1.04	2.13±0.35
		σ_η	3.01±0.54	3.01±0.72	2.73±1.83	2.56±1.73	2.39±0.95	2.93±0.43
no	3D	K_∞	$99.83^{+0.17}_{-0.24}$	$100.00_{-0.18}$	99.77±0.18	99.94±0.06	$99.95^{+0.05}_{-0.07}$	99.93±0.04
		p_{T_0}	4.73±0.01	4.70±0.02	4.61±0.03	4.52±0.04	4.45±0.06	4.62±0.01
		$\sigma_{p_{T0}}$	1.00±0.05	1.06±0.07	1.17±0.10	1.33±0.13	1.30±0.18	1.16±0.04
		C_η	3.12±0.57	2.33±0.51	1.38±0.50	1.82±0.66	0.90±0.48	1.80±0.21
		σ_η	3.38±0.50	2.82±0.37	2.79±1.00	2.04±0.43	2.88±0.82	2.90±0.25
	+2D	K_∞	$100.0_{-1.7}$	99.77±0.21	99.70±0.19	$100.0_{-0.4}$	$100.00_{-0.11}$	99.93±0.06
		p_{T_0}	4.78±0.01	4.73±0.02	4.64±0.03	4.54±0.05	4.41±0.08	4.67±0.01
		$\sigma_{p_{T0}}$	0.94±0.05	1.05±0.08	1.11±0.11	1.36±0.17	1.43±0.28	1.12±0.04
		C_η	3.83±0.66	2.21±0.59	1.92±0.73	1.31±0.51	1.06±0.57	1.98±0.25
		σ_η	3.21±0.38	3.05±0.67	2.39±0.88	3.09±0.73	2.84±0.90	3.06±0.31

Table 8: Results of the 5-parameter (Eq.5) fit of the XFT track finding efficiency for different requirements for electron and isolation for data sample B. K_∞ is measured in %, p_{T_0} in GeV/c , $\sigma_{p_{T0}}$ in $(100 \times \mathrm{GeV}/c)^{-1}$, C_η in $(0.1 \times \mathrm{GeV}/c)$ and σ_η in $0.1 \times$ $inversed\ units\ of\ rapidity$.

Ele.	ISO		number of prongs					
req.	type		1	2	3	4	5	any
yes	3D	K_∞	98.93±0.73	98.78±0.62	99.00±0.54	99.57±0.41	$99.85^{+0.15}_{-0.23}$	99.60±0.13
		p_{T_0}	4.88±0.02	4.81±0.02	4.75±0.03	4.62±0.04	4.58±0.06	4.74±0.01
		$\sigma_{p_{T0}}$	0.86±0.06	1.03±0.09	1.10±0.12	1.28±0.17	1.31±0.21	1.15±0.05
		C_η	9.03±1.19	6.66±1.13	6.79±1.21	4.12±1.04	2.06±0.85	5.85±0.44
		σ_η	3.55±0.46	3.31±0.59	3.43±0.63	3.87±0.81	3.72±1.61	3.45±0.24
	+2D	K_∞	99.25±0.70	98.78±0.57	98.81±0.56	99.16±0.53	$100.0_{-0.3}$	99.55±0.19
		p_{T_0}	4.89±0.02	4.83±0.02	4.74±0.04	4.63±0.05	4.55±0.09	4.79±0.01
		$\sigma_{p_{T0}}$	0.81±0.05	1.04±0.10	1.21±0.17	1.14±0.20	1.31±0.33	1.04±0.05
		C_η	9.42±1.23	7.68±1.34	6.41±1.43	4.23±1.36	2.25±0.91	6.11±0.51
		σ_η	3.87±0.49	2.90±0.51	3.06±0.62	3.39±0.90	4.34±1.22	3.59±0.30
no	3D	K_∞	98.41±0.53	98.91±0.49	98.96±0.39	99.57±0.31	$99.72^{+0.28}_{-0.33}$	99.53±0.11
		p_{T_0}	4.87±0.01	4.82±0.02	4.75±0.02	4.66±0.03	4.59±0.04	4.75±0.01
		$\sigma_{p_{T0}}$	0.90±0.05	1.00±0.06	1.14±0.09	1.25±0.11	1.33±0.16	1.12±0.03
		C_η	7.94±0.90	6.71±0.81	6.44±0.87	4.15±0.76	2.13±0.63	5.64±0.32
		σ_η	3.47±0.38	3.62±0.47	3.38±0.44	3.78±0.62	4.13±1.70	3.57±0.19
	+2D	K_∞	98.51±0.66	98.90±0.50	98.86±0.45	99.13±0.43	$99.95^{+0.05}_{-0.64}$	99.48±0.16
		p_{T_0}	4.90±0.01	4.85±0.02	4.75±0.03	4.65±0.04	4.54±0.06	4.79±0.01
		$\sigma_{p_{T0}}$	0.83±0.05	0.99±0.07	1.22±0.11	1.20±0.13	1.37±0.23	1.08±0.04
		C_η	9.31±1.07	7.23±0.93	6.08±0.98	4.21±0.95	2.66±0.79	5.95±0.38
		σ_η	3.65±0.40	3.46±0.47	3.45±0.50	3.53±0.76	4.44±1.13	3.76±0.24

Table 9: Results of the 5-parameter (Eq.5) fit of the XFT track finding efficiency for different requirements for electron and isolation for data sample C. K_∞ is measured in %, p_{T_0} in GeV/c , $\sigma_{p_{T0}}$ in $(100 \times \mathrm{GeV}/c)^{-1}$, C_η in $(0.1 \times \mathrm{GeV}/c)$ and σ_η in $0.1 \times$ $inversed\ units\ of\ rapidity$.

Ele.	ISO		number of prongs					
req.	type		1	2	3	4	5	any
yes	3D	K_∞	98.09±0.75	98.84±0.49	$99.75^{+0.25}_{-0.46}$	99.48±0.29	99.63±0.21	99.58±0.11
		p_{T_0}	4.88±0.01	4.81±0.02	4.75±0.02	4.63±0.04	4.43±0.08	4.74±0.01
		$\sigma_{p_{T0}}$	0.93±0.05	1.01±0.07	1.19±0.10	1.50±0.17	1.88±0.32	1.21±0.04
		C_η	8.95±1.03	6.48±0.94	5.20±0.77	3.82±0.87	2.22±0.87	5.55±0.35
		σ_η	3.28±0.42	3.52±0.42	4.41±0.83	3.38±0.68	2.82±0.82	3.45±0.20
	+2D	K_∞	98.20±0.75	98.32±0.65	$100.0_{-0.3}$	99.24±0.39	$99.85^{+0.15}_{-0.23}$	99.63±0.17
		p_{T_0}	4.89±0.01	4.83±0.02	4.78±0.03	4.62±0.05	4.47±0.10	4.80±0.01
		$\sigma_{p_{T0}}$	0.84±0.05	1.00±0.08	1.17±0.11	1.41±0.22	1.61±0.37	1.09±0.04
		C_η	10.13±1.12	6.70±1.08	6.19±0.88	4.46±1.17	3.59±1.14	6.22±0.41
		σ_η	3.42±0.40	3.89±0.53	4.45±0.49	2.82±0.87	2.95±0.75	3.89±0.25
no	3D	K_∞	98.69±0.46	98.76±0.36	99.48±0.29	99.42±0.25	99.62±0.21	99.55±0.09
		p_{T_0}	4.85±0.01	4.82±0.01	4.74±0.02	4.66±0.03	4.55±0.04	4.74±0.01
		$\sigma_{p_{T0}}$	0.96±0.04	1.01±0.05	1.19±0.07	1.38±0.10	1.49±0.15	1.19±0.03
		C_η	8.86±0.72	6.43±0.70	5.54±0.61	3.77±0.62	3.00±0.68	5.52±0.26
		σ_η	3.55±0.30	3.51±0.32	3.89±0.43	3.74±0.51	3.21±0.67	3.56±0.15
	+2D	K_∞	98.28±0.57	98.31±0.46	$99.75^{+0.25}_{-0.27}$	99.16±0.35	99.74±0.23	99.50±0.13
		p_{T_0}	4.89±0.01	4.85±0.01	4.76±0.02	4.66±0.03	4.55±0.05	4.79±0.01
		$\sigma_{p_{T0}}$	0.84±0.04	1.01±0.05	1.16±0.08	1.31±0.12	1.31±0.21	1.10±0.03
		C_η	10.57±0.90	6.44±0.80	6.49±0.70	4.20±0.76	4.05±0.89	6.23±0.31
		σ_η	3.37±0.29	3.76±0.38	3.93±0.38	3.57±0.63	3.11±0.56	3.72±0.17

8 Efficiency using the $W \to \tau\nu$ dataset

To cross-check the efficiency in the high-p_T region we use events from the tight $W \to \tau\nu$ sample [5] enriched with real taus (backgrounds are estimated to be less than 15%). These events were selected using the TAU_MET trigger with the following requirements for the tau-candidate: no extra jets with $E_T > 5$ GeV, fixed cone $10^o - 30^o$ tau tracking isolation, $p_{T\ tracks+\pi_0} > 30$ GeV/c, $\xi > 0.15$[3], $M(tracks + \pi_0) < 1.8$ GeV/c^2, calorimeter relative isolation $I_{R=0.4} < 0.1$. The sample has luminosity close to 50 pb^{-1} (around 2k events) and includes runs in the run number range from 141544 to 154050, but we consider only the runs before 152636, so we can compare it with data sample A and not incur a trigger bias[4].

We fit the $W \to \tau\nu$ data to a constant in the region $p_T > 6$ GeV/c because the data doesn't have enough events with low p_T τ's seed tracks, so it's hard to detect the turn-on region. Table 10 contains the results of this fit, and Figs. 9 and 10 show the efficiency dependencies on $1/p_T$ and on number of prongs. Though this sample gives large statistical uncertainties, especially for the number of prongs other then one or three, we can see that the results from it agree with ones from the jet data sample A.

It should be noted that when we require the tracks not to pass through the central COT spacer the efficiency becomes practically 100%, and the dips in the high-p_T region disappear.

Table 10: Results of the fit to a constant (in the region $p_T > 6$ GeV/c) of the XFT track finding efficiency for tau object's seed tracks for different requirements for isolation in the $W \to \tau\nu$ dataset. K_∞ is measured in %.

Iso type		number of prongs					
		1	2	3	4	5	any
3D	K_∞	97.3±1.3	95.7±2.4	99.3±0.7	$98.8^{+1.2}_{-1.7}$	$100.0_{-2.5}$	98.0±0.7
+2D	K_∞	97.4±1.2	96.2±2.4	98.9±0.9	$98.7^{+1.3}_{-1.8}$	$100.0_{-2.5}$	98.0±0.7

9 Conclusions

We have measured the XFT efficiency of the isolated track leg of the electron+track trigger as a function of p_T, η and the number of prongs around the seed track in 10^o cone. The efficiency found to be different for three run periods: (A) before run 152636, when the XFT allowed two missing hits per superlayer, (B) since run 152636 and before the Jan. 2003 shutdown (before run 156000), when only one missing hit was allowed, and (C) since the shutdown, when again one missing hit was allowed and the COT voltage was changed. After run 152636 the efficiency dropped considerably, and became p_T-dependent even in the high p_T region. For analyses we recommend using the 5-parameter fit results (Eq.(5)) obtained for the case when we apply 3D-tau-like isolation and require a loose electron partner (Tables 7, 8 and 9). For an estimation of the systematic uncertainties one may use the results with additional 2D isolation and with/without electron requirement.

[3] ξ is defined as $E_T^{had}/\Sigma p_T^{tracks}$ and effectively requires minimal hadronic energy associated with the available tracks.

[4] Starting run 152953 the requirement of an XFT track of $p_T > 10$ GeV/c was introduced for the TAU_MET trigger.

10 Acknowledgments

We thank Pasha Murat and Evelyn Thomson for help and useful discussions.

References

[1] M. Chertok *et al.*, CDF Note 4807.

[2] S. Baroiant *et al.*, CDF Note 6257.

[3] S. Baroiant *et al.*, CDF Note 6324.

[4] R. Hughes, E. Thomson and B. Winer, CDF Note 5986.

[5] P. Murat, CDF Note 6010.

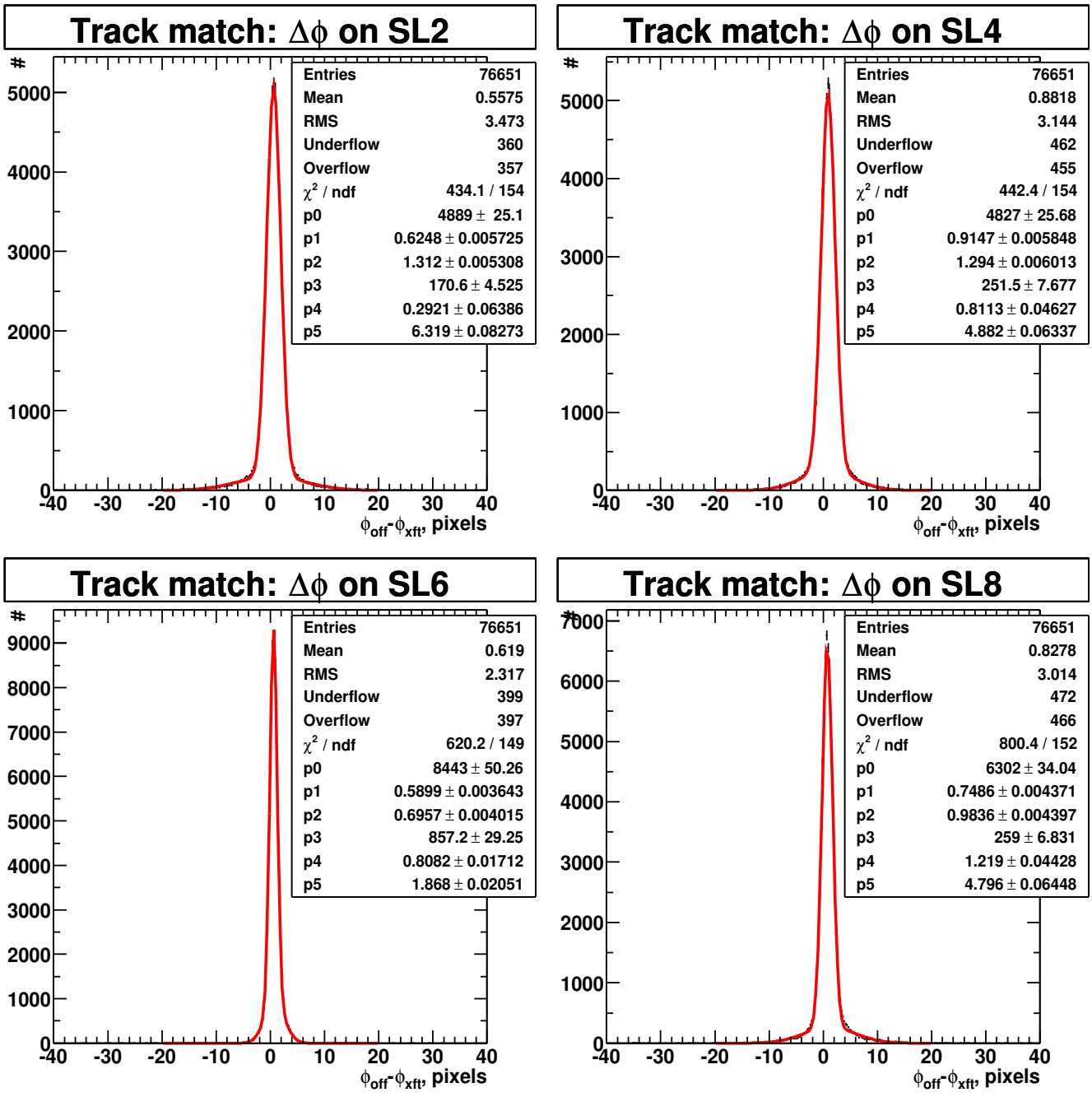

Figure 2: Distributions of the difference in ϕ between the offline track and its closest XFT partner on SL2, SL4, SL6 and SL8 for data sample A. The $\phi_{off} - \phi_{xft}$ is shown in number of pixels. Each distribution is fit to the sum of two Gaussians. They show that $|\Delta\phi| < 10$ pixels is a good matching interval.

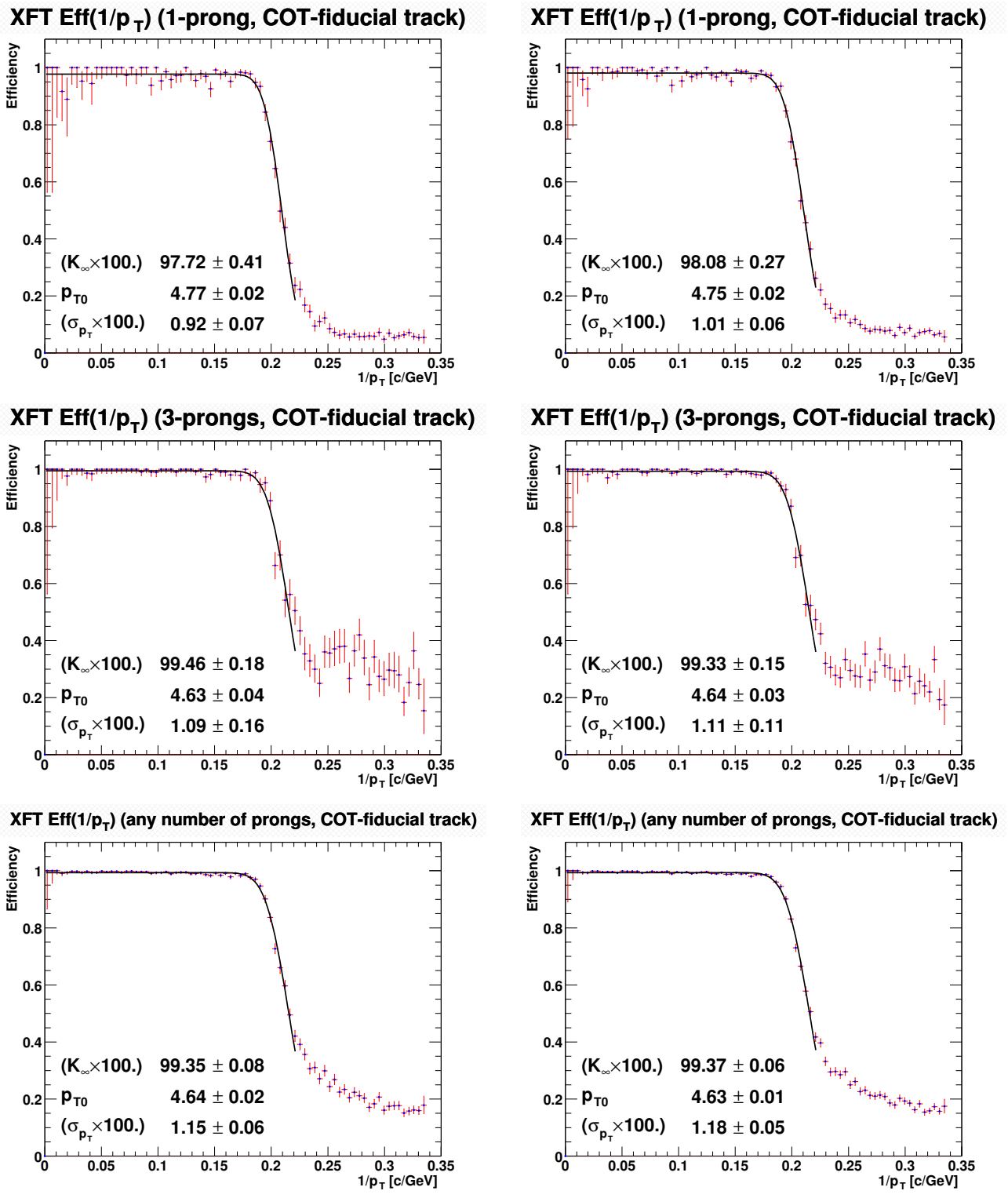

Figure 3: Results of the fit of the XFT track finding efficiency dependence on $1/p_T$ for the 1, 3 and any number of prongs (from the top to bottom) cases with (left) and without (right) electron requirement and 3D-tau-like isolation for data sample A.

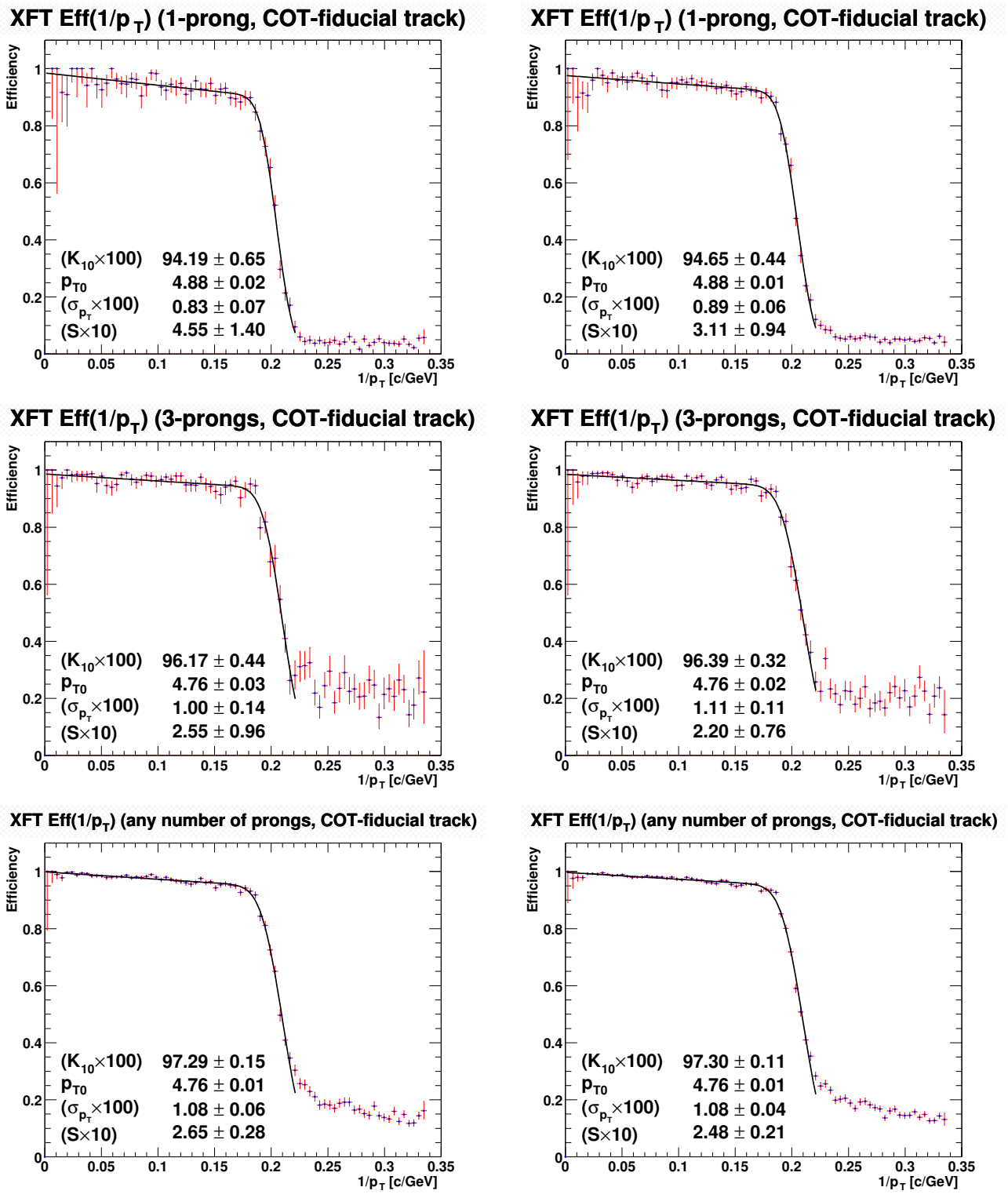

Figure 4: Results of the fit (with additional parameter for slope) of the XFT track finding efficiency dependence on $1/p_T$ for the 1, 3 and any number of prongs (from the top to bottom) cases with (left) and without (right) electron requirement and 3D-tau-like isolation for data sample B.

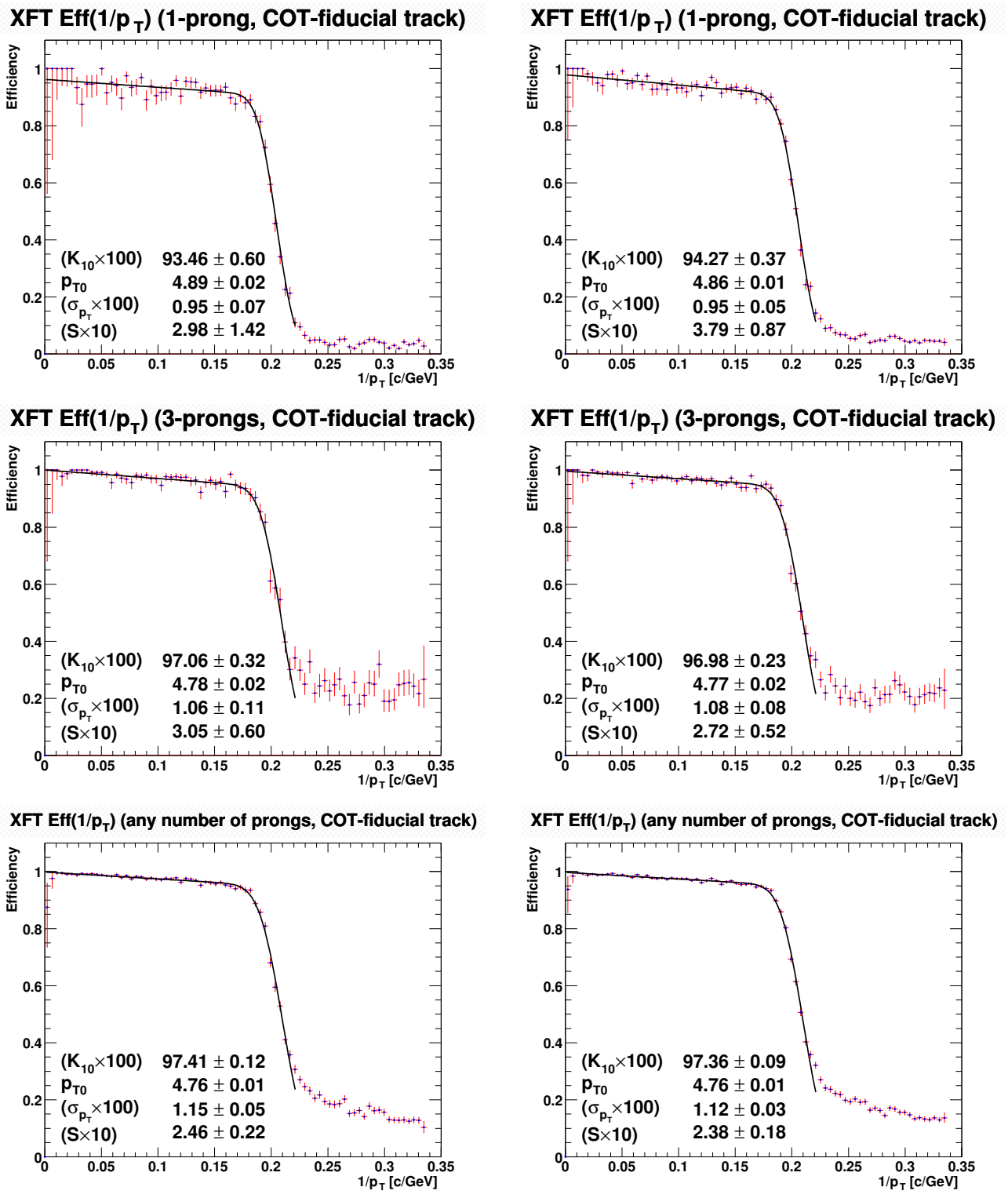

Figure 5: Results of the fit (with additional parameter for slope) of the XFT track finding efficiency dependence on $1/p_T$ for the 1, 3 and any number of prongs (from the top to bottom) cases with (left) and without (right) electron requirement and 3D-tau-like isolation for data sample C.

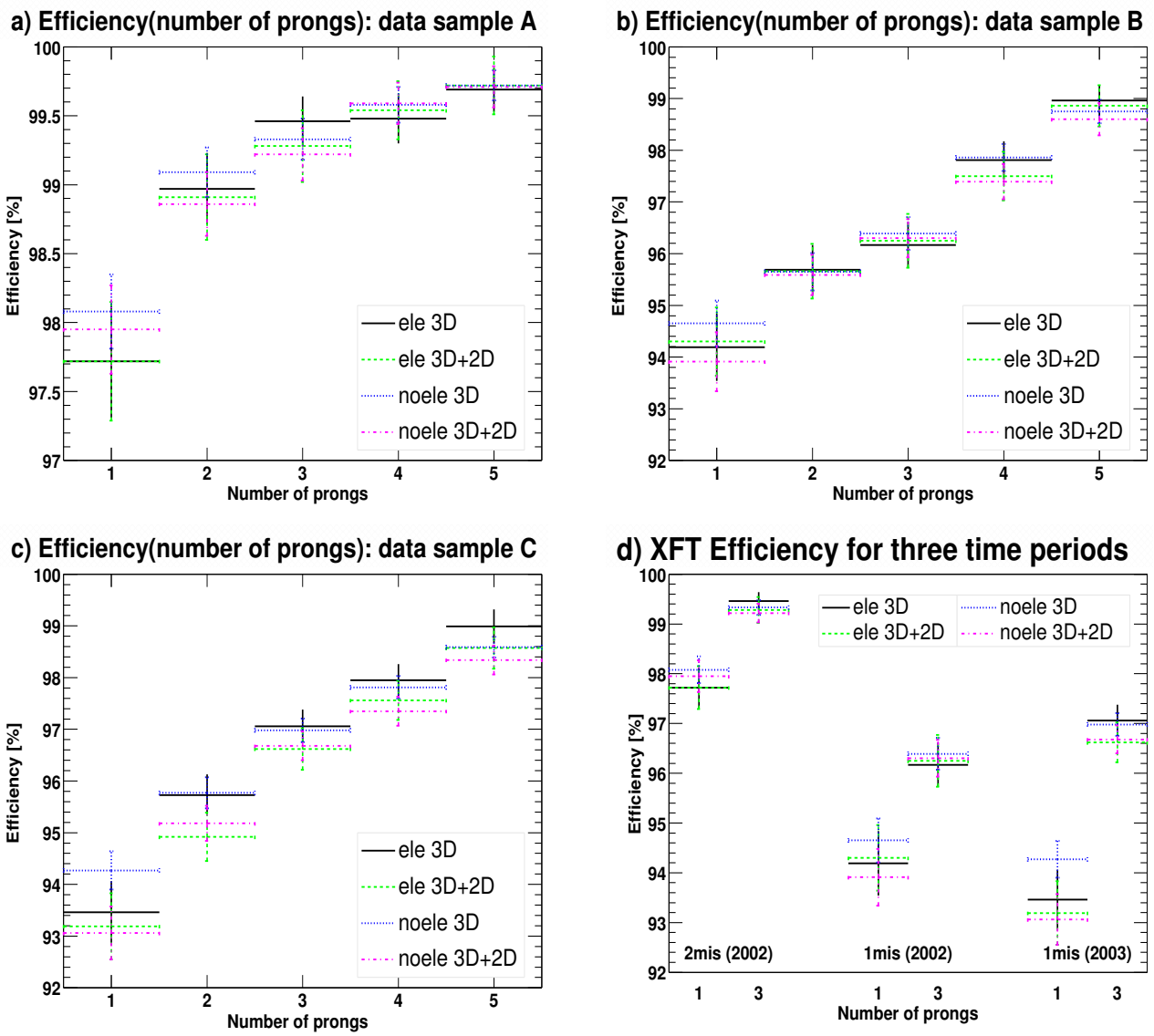

Figure 6: The XFT matching efficiency (depending on sample: at plateau or at $p_T = 10$ GeV/c) as a function of the number of tracks in a 10^o cone around the seed track for three data samples (plots a, b and c), and comparison of the efficiencies for tracks with 1 and 3 prongs for these samples (plot d), which correspond to the three periods with different XFT configuration (see Section 4). Each plot shows four combinations of track isolation and electron partner requirements.

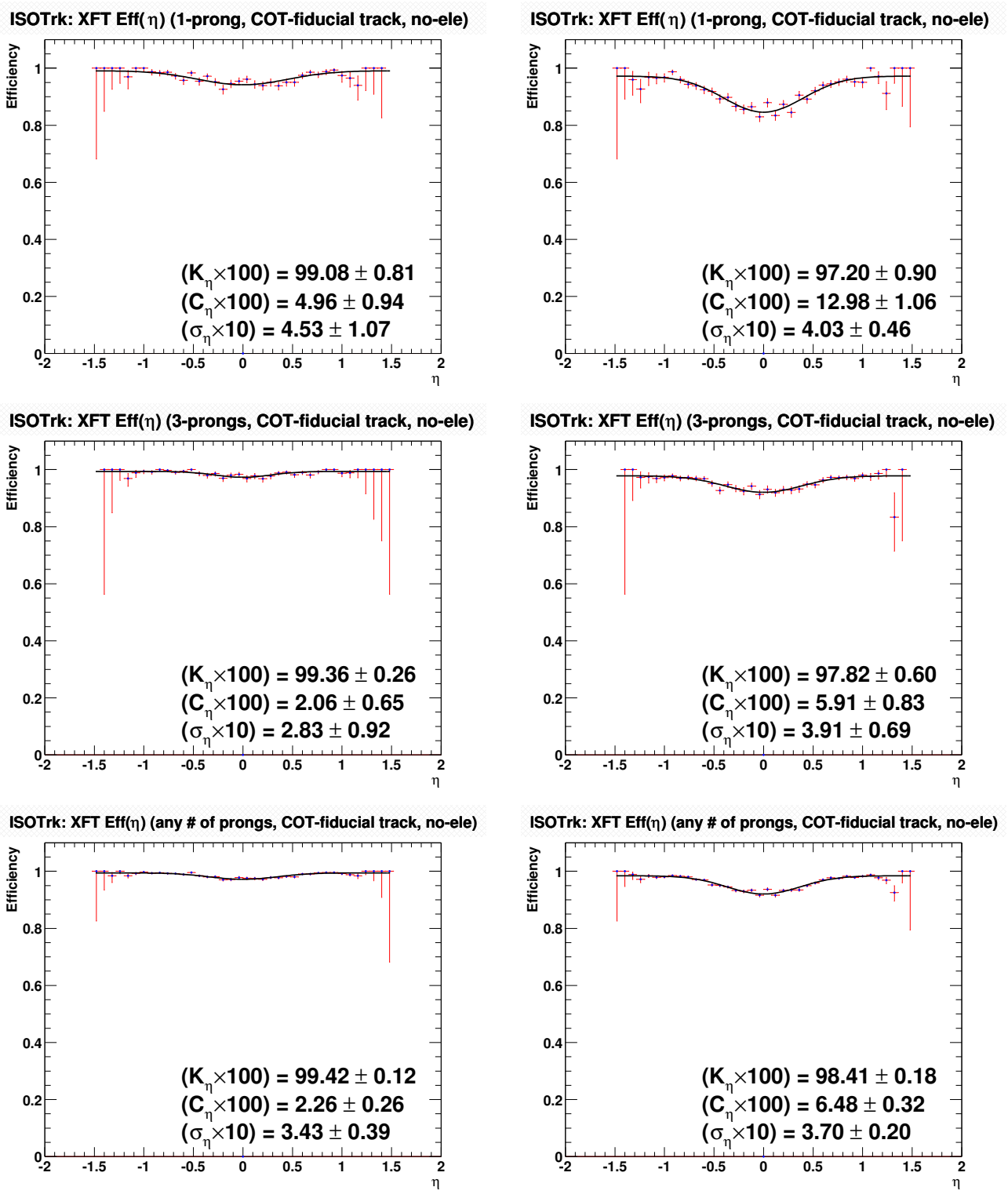

Figure 7: The XFT track finding efficiency dependence on η fit for different number of prongs wit electron partner requirement for data samples A (left) and C (right). The minimal offline track p_T was chosen to be $5\ \mathrm{GeV}/c$.

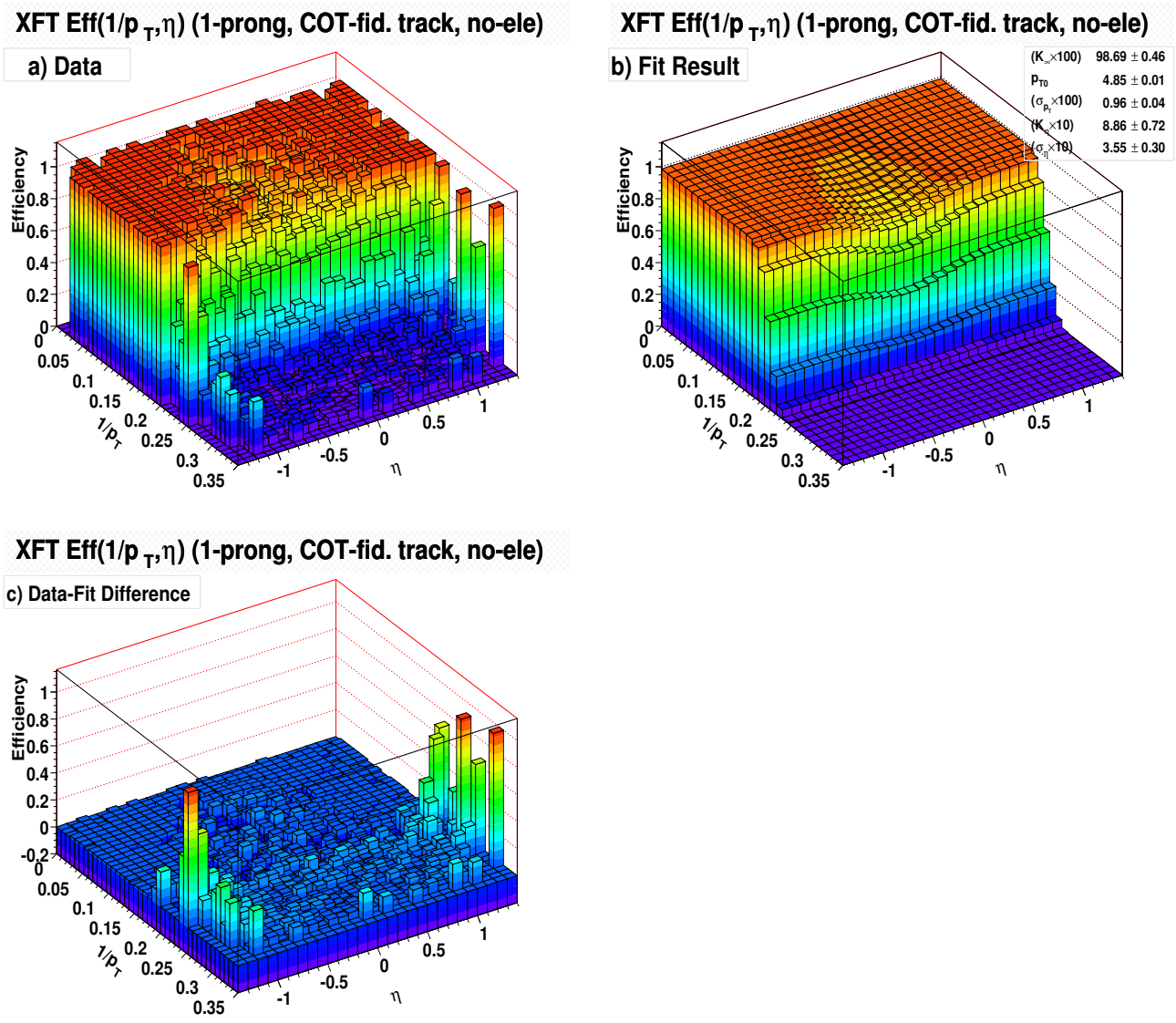

Figure 8: a) XFT track finding efficiency dependence on $1/p_T$ and η from data (1-prong case without electron requirement, 3D-tau-like isolation, data sample C), b) result of its 5-parameter fit, c) difference between data histogram and fit. From the plot c) we see that for some low p_T, high η regions the data-fit difference is high, which is explained by the fact that we do fitting for $0 < 1/p_T \lesssim 0.222$ GeV/c in order not to take into account the residual efficiency below the trigger threshold (see Section 2), and the statistics for the high η regions is low.

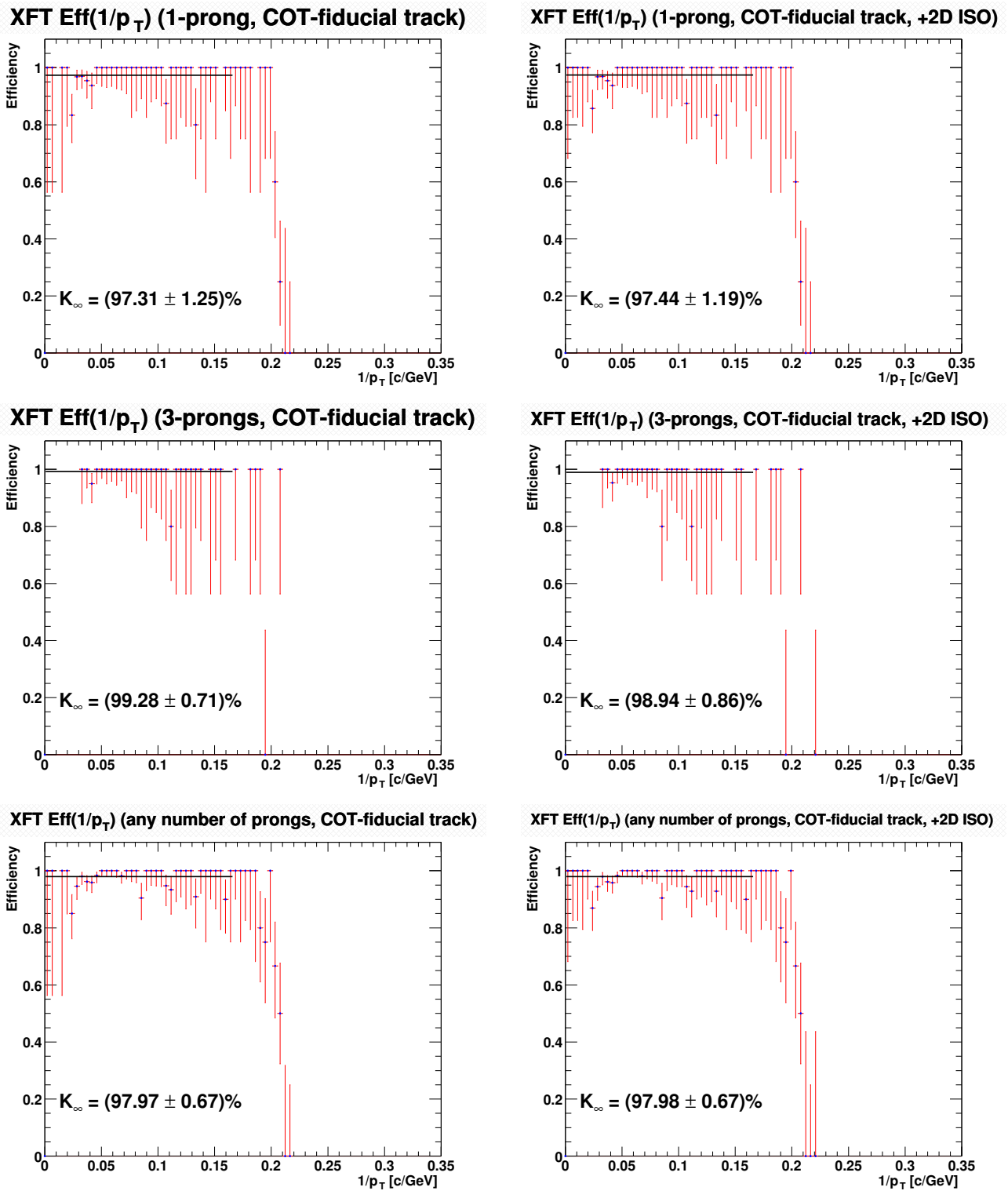

Figure 9: Results of the fit to a constant (in the region $p_T > 6$ GeV/c) of the XFT track finding efficiency dependence on $1/p_T$ for the 1, 3 and any number of prongs (from the top to bottom) cases with usual 3D-tau-like isolation (left) and with additional 2D isolation (right) for the $W \to \tau\nu$ dataset.

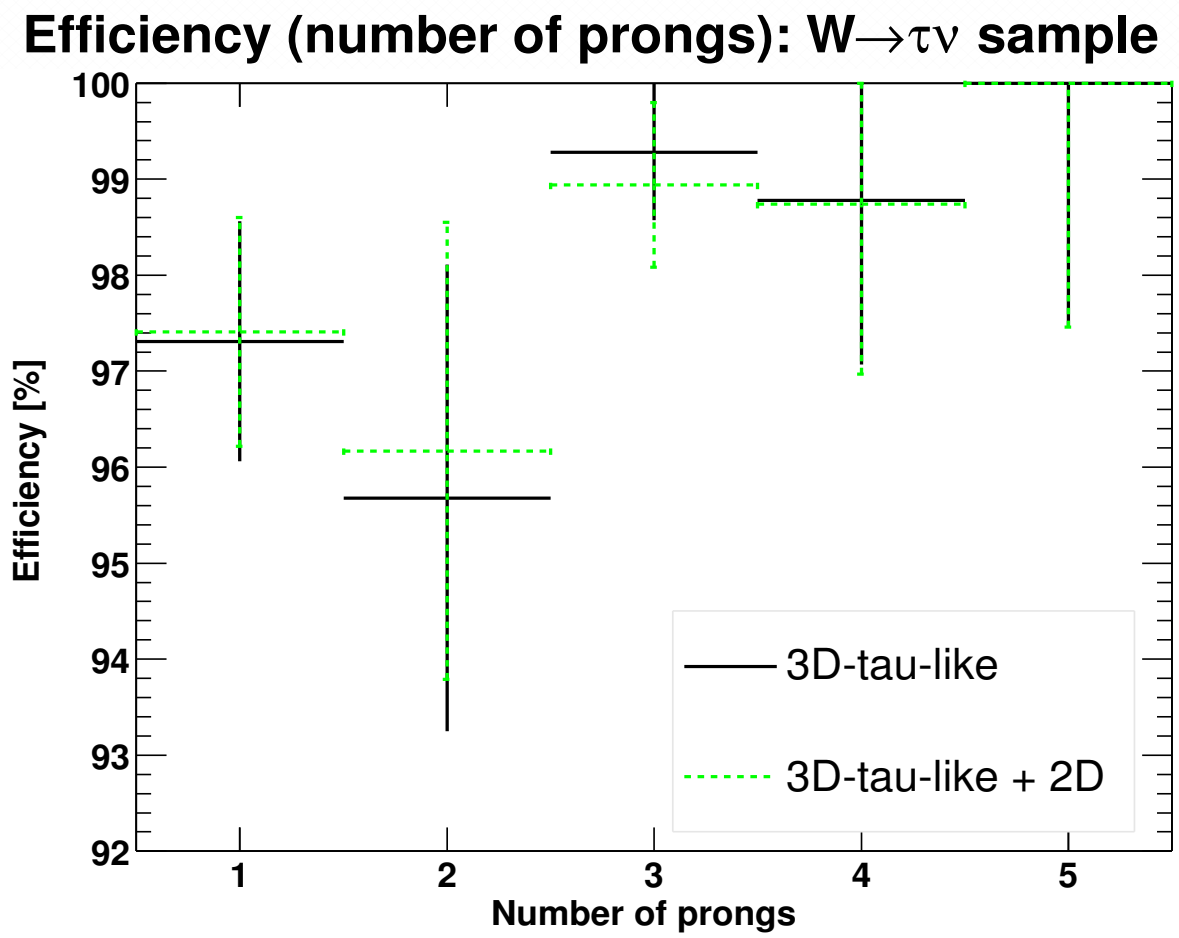

Figure 10: XFT matching efficiency as a function of the number of tracks in 10^o cone around seed track for the $W \rightarrow \tau\nu$ dataset. Two different cases of track isolation are shown.